Stable Isotope Probing and Raman Spectroscopy for Monitoring Carbon Flow in a Food Chain and Revealing Metabolic Pathway

ARTICLE *in* ANALYTICAL CHEMISTRY · DECEMBER 2012

Impact Factor: 5.64 · DOI: 10.1021/ac302910x · Source: PubMed

5 AUTHORS, INCLUDING:

Mengqiu Li
University of Leeds
11 PUBLICATIONS **145** CITATIONS
SEE PROFILE

Wei E Huang
University of Oxford
86 PUBLICATIONS **1,325** CITATIONS
SEE PROFILE

Alexandre Jousset
Utrecht University
37 PUBLICATIONS **589** CITATIONS
SEE PROFILE

analytical chemistry

Article

pubs.acs.org/ac

Stable Isotope Probing and Raman Spectroscopy for Monitoring Carbon Flow in a Food Chain and Revealing Metabolic Pathway

Mengqiu Li,[†] Wei E. Huang,*[,†] Christopher M. Gibson,[‡] Patrick W. Fowler,[‡] and Alexandre Jousset[§]

[†]Department of Civil and Structural Engineering, Kroto Research Institute, North Campus, The University of Sheffield, Broad Lane, Sheffield S3 7HQ, U.K.

[‡]Department of Chemistry, The University of Sheffield, Sheffield S3 7HF, U.K.

[§]J.F. Blumenbach Institute of Zoology and Anthropology, University of Göttingen, Berliner Str. 28, 37073 Göttingen, Germany

Supporting Information

ABSTRACT: Accurately measuring carbon flows is a challenge for understanding processes such as diverse intracellular metabolic pathways and predator-prey interactions. Combined with stable isotope probing (SIP), single-cell Raman spectroscopy was demonstrated for the first time to link the food chain from carbon substrate to bacterial prey up to predators at the single-cell level in a quantitative and nondestructive manner. *Escherichia coli* OP50 with different ^{13}C content, which were grown in a mixture of ^{12}C- and fully carbon-labeled ^{13}C-glucose (99%) as a sole carbon source, were fed to the nematode. The ^{13}C signal in *Caenorhabditis elegans* was proportional to the ^{13}C content in *E. coli*. Two Raman spectral biomarkers (Raman bands for phenylalanine at 1001 cm^{-1} and thymine at 747 cm^{-1} Raman bands), were used to quantify the ^{13}C content in *E. coli* and *C. elegans* over a range of 1.1−99%. The phenylalanine Raman band was a suitable biomarker for prokaryotic cells and thymine Raman band for eukaryotic cells. A biochemical mechanism accounting for the Raman red shifts of phenylalanine and thymine in response to ^{13}C-labeling is proposed in this study and is supported by quantum chemical calculation. This study offers new insights of carbon flow via the food chain and provides a research tool for microbial ecology and investigation of biochemical pathways.

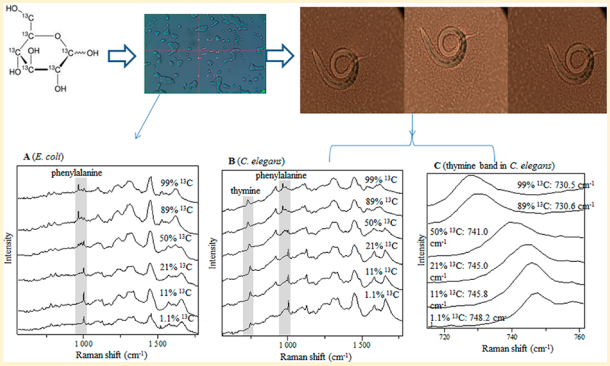

Combination of stable isotope probing (SIP) with Raman spectroscopy has been proven to be a novel and valuable approach in microbiology, microbial ecology, and clinical research.[1−6] Single-cell Raman spectra of living organisms are signatures or "fingerprints" of their intrinsic chemical composition which indicate the metabolic profile, phenotypic features, and physiological status of the sample.[1,2] The SIP-Raman method has been used to determine bacterial species involved in biodegradation processes, reveal extracellular activity of a human pathogen, and quantify carbon dioxide fixation at a single-bacterium level.[3,6−8] The SIP-Raman method can potentially track carbon flow in a complex community in a quantitative and nondestructive manner. This study demonstrates that the SIP-Raman method can track carbon flow quantitatively in a model food chain that consists of an organic carbon source, bacteria, and soil nematodes. From detailed examination of spectral data, it is shown that the SIP-Raman method can provide another layer of information regarding the biochemical pathways that lead to the synthesis of crucial biological molecules. This study brings new insights about carbon flow via a food chain and brings a novel research tool to microbial ecology and the investigation of biochemical pathways.

Soil bacteria form the basis of soil food webs and drive numerous soil processes, such as nutrient turnover, phytohormone production, and pathogen suppression.[9] In the rhizosphere, bacteria are top-down regulated, and predation has important consequences on the structure and functioning of the microbial community.[10] Nematodes are among the main consumers of bacteria in terrestrial ecosystems. Understanding the nutrient flows between bacteria and nematodes is of central importance for the reconstruction of soil food webs and reliable prediction of nutrient cycles. Recently, SIP has revolutionized research on predator−prey interactions in soil, allowing the fate of ^{13}C-labeled substrates to be followed into bacteria, protozoa, and meso- and macrofauna.[11−14] Most SIP experiments identify microorganisms by fractionating heavier ^{13}C-labeled nucleic acid using ultracentrifugation.[8,15] This method has greatly enriched our knowledge of microbial communities and can be used, for example, to investigate active root-associated communities and uncover the complex links between bacteria, fungi, and protozoa.[11,16] However, this nucleic acid-based SIP is destructive, time-consuming, and requires a high degree of

Received: October 6, 2012
Accepted: December 22, 2012

dx.doi.org/10.1021/ac302910x | *Anal. Chem.* XXXX, XXX, XXX−XXX

labeling (usually more than 50% ^{13}C) to ensure efficient separation of ^{13}C- from ^{12}C-nucleic acids and would therefore miss organisms that incorporate the labeled substrate less quickly or grow at a slower rate. In contrast, Raman spectroscopy is nondestructive and rapid (a few seconds per single cell). As shown in this study, it also detects ^{13}C labeling over almost the entire range from 1.1 to 99%. To the best of our knowledge, it is the first to link the food chain from carbon substrate to consumers (bacterial prey) and predators at the single-cell level.

The detection of ^{13}C incorporation is achieved by measuring the isotopic shift ("red shift" of Raman bands) caused by the slightly heavier ^{13}C-atoms. Raman red shift was observed in single cells at many positions across the spectra which correspond to amide, nucleobases, phenylalanine, etc.; red-shifted bands are potential quantitative spectral markers for ^{13}C content of the sample.[1] However, owing to the complex nature of cells, many of the red-shifted Raman bands overlap with other bands and therefore Raman spectral markers that can be used for ^{13}C content quantification are limited.

The Raman band of phenylalanine is a well-established marker for ^{13}C incorporation at the single-cell level.[7] It is a sharp band at about 1001 cm^{-1} with limited interference from other Raman bands. It is observed almost in any type of cell. In this study, we report a new quantitative Raman spectral marker for ^{13}C in single nematodes. This marker appears at about 747 cm^{-1} in ^{12}C-nematode samples, and it was assigned to thymine. The different isotopic-shift patterns of phenylalanine and thymine Raman bands arise from their different biosynthetic pathways, thus revealing a new link between Raman spectra and biochemical pathways.

MATERIALS AND METHODS

Bacteria Strain and Growth Conditions. *Escherichia coli* OP50 was maintained on lysogeny broth (LB) agar plates at 37 °C. Prior to the experiment, one colony was picked and grown overnight in OS minimal medium[17] supplemented with a mixture of ^{12}C- and ^{13}C-glucose (both from Sigma-Aldrich Company, U.K.) as the sole carbon source. We set up an isotopic gradient comprising 1.1 (natural abundance), 2.1, 6.0, 11, 21, 50, 89, and 99% ^{13}C, at a total concentration of 25 mM glucose. To ensure reliable labeling, bacteria were grown overnight, and a 100 μL aliquot was used to start a new 10 mL culture at the same isotopic ratio. Bacteria were then pelleted by centrifugation (16000 g, 2 min), washed three times in M9 buffer to remove remaining nutrients, and concentrated in 50 μL M9 buffer. M9 plates without carbon were seeded with the labeled *E. coli* and kept at 4 °C until the start of the experiment.

Nematodes and Growth Conditions. *Caenorhabditis elegans* were routinely grown in NGM plates seeded with *E. coli* OP50. Prior to the experiments, eggs were scraped down the plate, sterilized with 1% NaClO for 5 min, and washed according to standard procedures. About 50 eggs were placed on each agar plate (three plates for each isotopic ratio and time point) and incubated at 20 °C in the dark. After 5, 10, 15, and 20 days, nematodes were washed off the plates with 1 mL M9 buffer; the worms were collected by gentle centrifugation (20*g*, 1 min) and washed three times with M9 buffer to remove bacteria. The worms were then fixed in 1% formaldehyde and analyzed by Raman microspectroscopy, as described below.

Raman Microspectroscopy. Each nematode or bacterial suspension (5−10 μL) was spread on a calcium fluoride slide and allowed to air-dry prior to Raman analysis. Raman spectra were acquired using a confocal Raman microscope (LabRAM HR, HORIBA Scientific, U.K.) equipped with an integrated Olympus microscope (model BX41). A 100× magnifying dry objective (NA = 0.90, Olympus, U.K.) was used to observe samples and acquire Raman signals. The laser beam was targeted on samples visually using an integrated camera and a motorized *XYZ* stage (0.1 μm step). Raman scattering was excited with a 532 nm Nd:YAG laser (Torus Laser, Laser Quantum, U.K.). The laser power on a sampling point was about 3.5 mW. Raman spectra were recorded by a −70 °C-cooled CCD detector (Andor, U.K.). The system was run with a confocal pinhole diameter of 100 μm, enabling a spatial resolution of approximately 1 μm. Each Raman spectrum was acquired in the range of 557 and 2172 cm^{-1}, with 1021 data points and a spectral resolution of about 1.5 cm^{-1}. LabSpec software (HORIBA Scientific, U.K.) was used to control the Raman system and acquire spectra. Acquisition times of Raman spectra were 5−10 s for nematodes and 30 s for bacteria. In each nematode sample, a few worms were randomly chosen and measured at multiple points along their bodies. Smoothing of spectra was performed by the Savitsky−Golay smoothing method in LabSpec. Microsoft Excel 2007 was used to process and analyze spectral data.

Calculation of the Wavenumbers of Phenylalanine Raman Bands and Thymine Raman Spectra. The equilibrium geometry of the phenylalanine molecule was obtained at the B3LYP/6-31G** level of theory using GAUSSIAN09.[18] Raman frequencies of phenylalanine were calculated in the harmonic approximation for the isotopomers 1 to 8 derived by $^{12}C/^{13}C$ substitution (Figure S4 of the Supporting Information). The structure of thymine was optimized and checked using the same procedure. The Raman frequencies and intensity constants of the 32 possible isotopomers of thymine (Figure S6 of the Supporting Information) derived by $^{12}C/^{13}C$ substitution were calculated using the same method. The thymine Raman band was calculated by superposition of the 32 possible isotopomers of thymine. Each isotopomer was treated as an individual Raman band, and these 32 bands were simulated using both Gaussian and Lorentzian line shape functions.

The probability P_i of a given isotopomer, i, of thymine was calculated using the following function:

$$P_i = (1 - p)^{5-z_i} p^{z_i} \quad (1)$$

where p is the fractional ^{13}C content ($0 \le p \le 1$) and z_i is the number of ^{13}C atoms in the isotopomer.

Any isotopomer, i, has a calculated Raman frequency, b_i, and an intensity constant, E_i. The full width at half-maximum (fwhm) was set to equal that of the observed thymine Raman bands at 1.1% and 99% ^{13}C, which is about 12 cm^{-1}. For any isotopomer, i, of thymine, the Gaussian function representing the individual Raman band is

$$G_i(x) = a_i\, e^{-(x-b_i)^2/2c^2} \quad (2)$$

where

$$c = \frac{\mathrm{FWHM}}{2\sqrt{2 \ln 2}} \quad (3)$$

If we assume that

$$\int_{+\infty}^{-\infty} G_i(x)\, \mathrm{d}x = P_i E_i \quad (4)$$

dx.doi.org/10.1021/ac302910x | Anal. Chem. XXXX, XXX, XXX−XXX

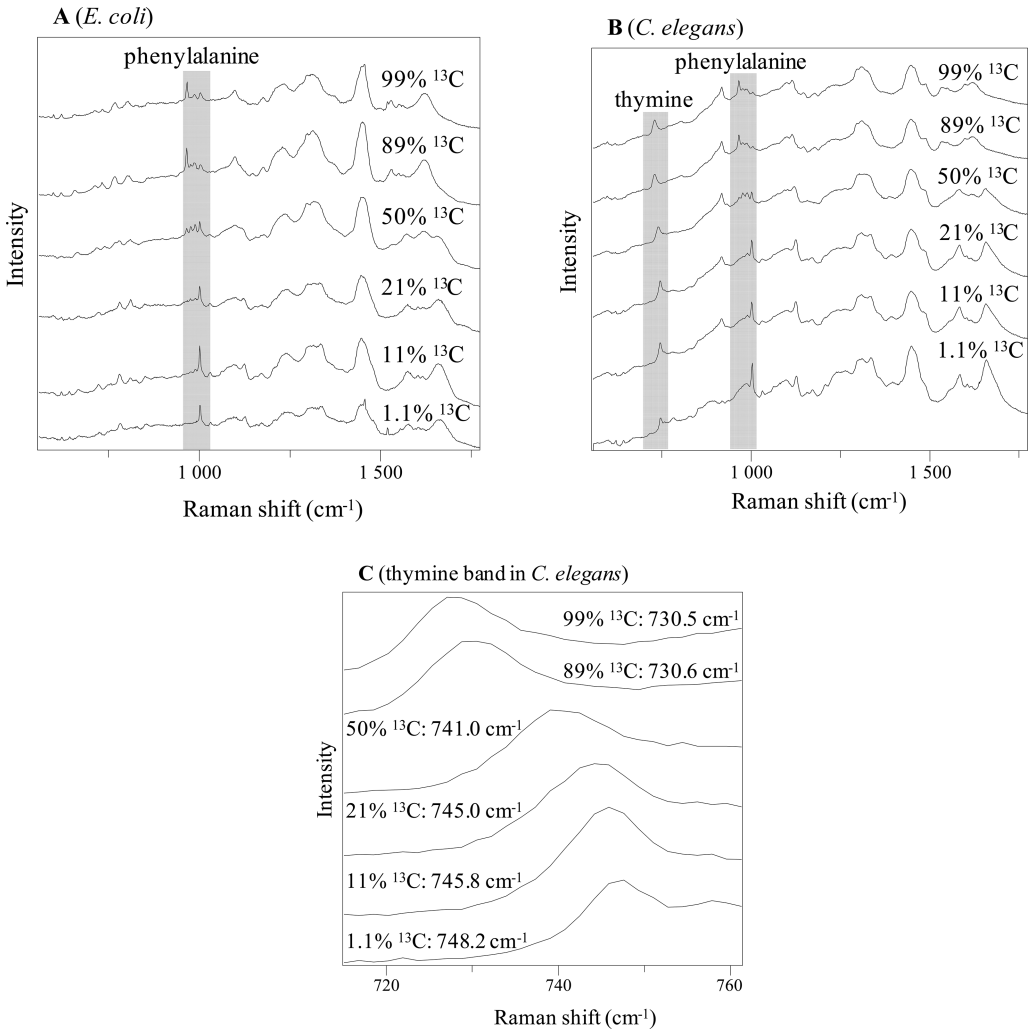

Figure 1. Examples of Raman spectra of ^{13}C-labeled (A) *E. coli* and (B) *C. elegans* fed by the labeled *E. coli*. (A and B) Shaded areas are the red-shifted phenylalanine and thymine bands; (C) the gradual red shift of the thymine band can potentially quantify ^{13}C content of *C. elegans*.

and note that the integral of the Gaussian function is

$$\int_{+\infty}^{-\infty} G_i(x)\,dx = a_i c\sqrt{2\pi} \tag{5}$$

the pre-exponential factor is

$$a_i = \frac{P_i E_i}{c\sqrt{2\pi}} \tag{6}$$

Similarly, the Lorentzian function representing the Raman band of isotopomer i is

$$L_i(x) = \frac{d_i \frac{\mathrm{FWHM}}{2}}{\pi\left[(x-b_i)^2 + \left(\frac{\mathrm{FWHM}}{2}\right)^2\right]} \tag{7}$$

If we assume that

$$\int_{+\infty}^{-\infty} L_i(x)\,dx = P_i E_i \tag{8}$$

and note that the integral of the Lorentzian function is

$$\int_{+\infty}^{-\infty} L_i(x)\,dx = d_i \tag{9}$$

we derive

$$d_i = P_i E_i \tag{10}$$

Finally, Raman spectra of thymine at six ^{13}C levels (p = 1.1, 11, 21, 50, 89, and 99%) were simulated using either

$$\mathrm{Raman}(x)_p = \sum_{32}^{i=1} G_i(x) \tag{11}$$

or

$$\mathrm{Raman}(x)_p = \sum_{32}^{i=1} L_i(x) \tag{12}$$

Simulated Raman spectra based on both Gaussian and Lorentzian functions were plotted using Microsoft Excel 2007 (Figure 5, panels A and B).

RESULTS

Using Raman Red Shift to Track Carbon Flow in a Model Predator–Prey System. In this study, *E. coli* were labeled with 1.1 (natural abundance of ^{13}C) to 99% ^{13}C by growing them on ^{13}C-labeled glucose. ^{13}C-labeled bacteria were then fed to the nematode model strain *Caenorhabditis elegans*. It has been previously demonstrated that Raman spectroscopy is a reliable, quantitative, and rapid method to detect carbon flow

dx.doi.org/10.1021/ac302910x | Anal. Chem. XXXX, XXX, XXX–XXX

from carbon substrates to single bacteria cells.[3,6] ^{13}C labeling of bacteria from 1.1 to 99% was shown in Figure 1A. As shown in Figure 1B, Raman spectra of nematodes fed by ^{13}C bacteria have distinctive "red shifts" similar to that of bacteria.[1] This result indicates that monitoring Raman spectra of single nematodes is a good measurement for ^{13}C incorporation at the single-organism level and can therefore track the nutrition flow from the carbon source, via microbial cells (prey), up to multicellular predators.

Many Raman bands in the spectra of nematodes are visibly red-shifted, but the majority of them also overlap with other bands. In this study, only phenylalanine and thymine bands (shaded areas in Figure 1B) are readily useful for quantifying ^{13}C content in *C. elegans*. However, a broad and strong band appeared close to the phenylalanine band (1001 cm^{-1}). This unidentified band could be significantly reduced by photobleaching using the Raman probing laser in about 10 s, but a raised baseline with a rounded shape is still seen in the shaded area of phenylalanine in Figure 1B. This interfering band possibly arises from autofluorescence or the fixation procedure for nematode samples. In order to correlate the phenylalanine band with ^{13}C content, the intensity of phenylalanine band must be derived from baseline-corrected Raman spectra. Baseline correction of Raman spectra is usually done by so-called "rubber-band" baseline subtraction, which is arbitrary and introduces unnecessary uncertainties. Because of the difficulties listed above, the correlation between the red shift of the phenylalanine band and the ^{13}C content is relatively weak (with R^2 values <0.9 in linear regression) and unreliable because it was calculated from heavily processed spectra which still contain the unidentified interfering band.

In contrast, the thymine Raman band, the new quantitative ^{13}C spectral marker reported in this study, overcomes all the problems associated with the phenylalanine band. It peaks at about 747 cm^{-1} in ^{12}C-nematode samples (with 1.1% natural abundance of ^{13}C) and has been assigned to thymine in a number of studies.[19−25] Raman spectra of deoxynucleotides (dATP, dTTP, dGTP, and dCTP, 100 mM, Sigma-Aldrich) also support this band assignment (Figure S1 of the Supporting Information). The thymine Raman band moves gradually to a lower wavenumber with increasing ^{13}C content (Figure 1C). Therefore, by finding the position of the thymine band of a nematode sample, one can determine the extent of ^{13}C incorporation quantitatively, without using the band intensity.

If a statistically sound relationship can be established between the position (wavenumber) of the thymine band and the ^{13}C content, one can use it to determine the ^{13}C content of a single organism based on the nondestructive and easy-to-use technique of Raman spectroscopy. As shown in Figure 2, linear regression results in a good linear relationship between the position of the thymine band and the ^{13}C content in single *C. elegans*. In samples that underwent 5, 10, and 15 days of incubation, R^2 values are 0.95−0.97. Therefore, quantitative detection of ^{13}C incorporation ranging from 1.1 to 99% in *C. elegans* can be achieved at the single-organism level. As previously shown, the ^{13}C content of a biological molecule is a good quantitative indicator for the ^{13}C content of the whole cell.[3] A *t* test indicated that the Raman shift of the thymine band is significant to *C. elegans* which were fed with 21% ^{13}C-labeled *E. coli* cells (Table S1 of the Supporting Information).

It is worth noting that the thymine band has a very different "red-shift pattern" from the previously described phenylalanine band.[7] A ^{13}C-phenylalanine band at about 965 cm^{-1} appears

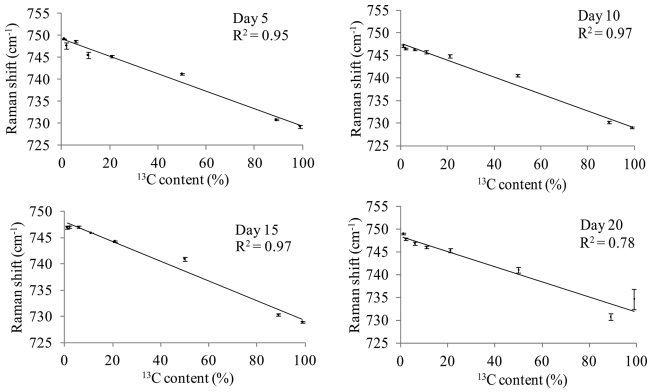

Figure 2. The linear relationship between the position (wavenumber) of the thymine Raman band and ^{13}C content of *C. elegans*. Error bars show the standard error of Raman band positions at each ^{13}C level.

from fully ^{13}C-labeled cells. The ^{12}C-phenylalanine band at about 1001 cm^{-1} does not disappear or move in the presence of ^{13}C; instead, with increasing ^{13}C content, it loses intensity as the ^{13}C-phenylalanine band gains intensity. Therefore, ^{13}C content can be correlated to the ratio or difference between these two intensities. In addition, we observed two extra Raman bands between the ^{13}C-phenylalanine band and the ^{12}C-phenylalanine band in *E. coli* grown in 50% ^{13}C media (Figure 3A); in these spectra, all four bands have almost identical intensities. A similar four-band feature has been observed previously.[7]

For thymine, however, no new band was observed from ^{13}C-labeled samples. The thymine band moves gradually toward the lower wavenumbers with increasing ^{13}C content (Figures 1C and 2). In the entire range of ^{13}C % used in this study, there was always only one thymine band, without obvious band splitting.

We hypothesize that this difference in red-shift pattern results from different biosynthetic pathways of phenylalanine and thymine. There are a large number of phenylalanine and thymine molecules in living cells; in any given molecule of phenylalanine or thymine, each carbon atom can be ^{12}C or ^{13}C, resulting in different isotopomers. There are 9 and 5 carbon atoms in phenylalanine and thymine, respectively. If we allow for free rotation of the aromatic ring about its σ bond with the "alanine" moiety, there are 320 ($2^9 - 12 \times 2^4$) different isotopomers for phenylalanine. Thymine has 32 (2^5) different isotopomers. Phenylalanine and thymine are synthesized by particular pathways, and so the number of permitted isotopomers may be smaller than the theoretical upper bounds of 320 and 32 for phenylalanine and thymine, respectively. Each isotopomer has, in principle, a different Raman frequency (usually reported as a wavenumber). A Raman spectrum of a single bacterium or part of a nematode contains contributions from all molecules within its focal point, and each detected molecule may be any one of the permitted isotopomers. We can reasonably assume that every molecule contributes equally to the spectrum. Therefore, the shape of a Raman band encodes the shape of the probability distribution of the isotopomers, and the observed difference in the red-shift pattern of phenylalanine and thymine indicates that their probability distributions of isotopomers may have very different shapes.

Proposed Mechanism for the Red-Shift Pattern of the Phenylalanine Raman Band. In order to determine the

dx.doi.org/10.1021/ac302910x | *Anal. Chem.* XXXX, XXX, XXX−XXX

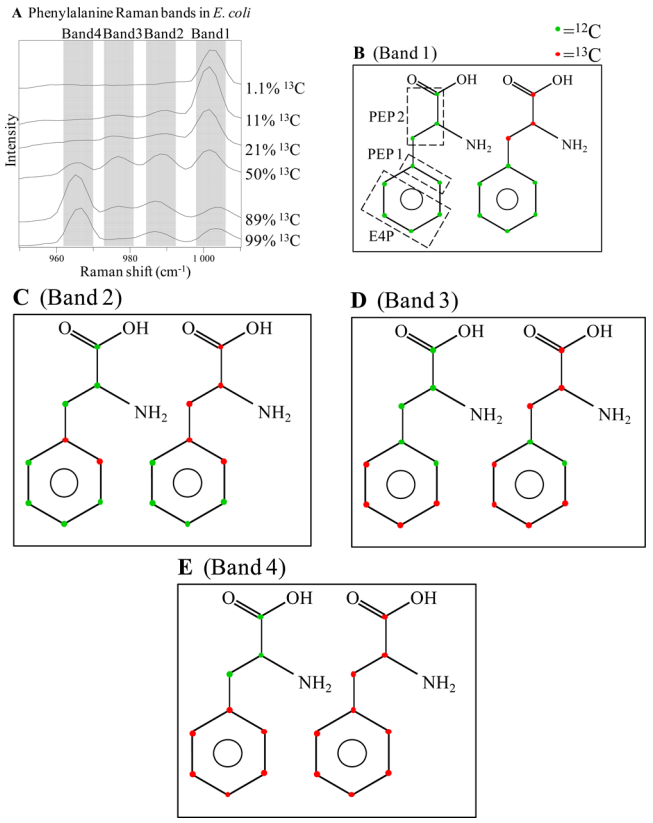

Figure 3. The assignment of the four phenylalanine Raman bands. Four phenylalanine Raman bands were observed in *E. coli*, including (A) the full ^{12}C band (Band 1) and the full ^{13}C band (Band 4). There are eight permitted isotopomers of phenylalanine; they are assigned to (B–E) the four Raman bands. The origin of carbon atoms is shown in (B).

permitted isotopomers of phenylalanine, we can start tracking carbon atoms from glycolysis. The flow of carbon atoms in the biosynthesis of phenylalanine is shown in Figure S2 (panel A) of the Supporting Information.[26] Although phenylalanine may be synthesized from other precursors by different reactions, in our experiments glucose was the sole carbon source, and Raman spectra are usually taken shortly after the start of incubation; it is reasonable to assume that the biosynthesis of phenylalanine mainly relies on the input of carbon atoms from glycolysis. One glucose 6-phosphate (G6P) molecule and two phosphoenolpyruvate (PEP 1 and PEP 2) molecules provide carbon atoms to the biosynthesis of phenylalanine. Erythrose 4-phosphate (E4P) inherits four carbon atoms from G6P. One carbon atom that originates from a PEP molecule is removed during the synthesis ("PEP 1" in Figure 3B and Figure S2, panel A of the Supporting Information). Therefore, E4P, PEP 1, and PEP 2 provide four, two, and three carbon atoms to phenylalanine, respectively. The destination of the carbon atoms is shown in Figure 3B. As seen in Figure 3B, E4P, PEP 1, and PEP 2 provide three "modules" to form phenylalanine, and glucose is the common precursor of all three modules. Since a mixed glucose (fully labeled ^{12}C- or ^{13}C-glucose in different proportions) source was given as the sole carbon source, each one of the E4P, PEP 1, and PEP 2 molecules randomly picks up all ^{12}C or all ^{13}C. The isotopic composition of E4P, PEP 1, and PEP 2 should therefore be independent of each other. Therefore, the number of permitted isotopomers of phenylalanine is $2^3 = 8$. These isotopomers are shown in Figure 3 (panels B–E). The aromatic ring of phenylalanine, however, has only four isotopic forms. The phenylalanine Raman band corresponds to an aromatic ring vibrational mode, and therefore, the key atoms that affect its Raman frequency are those in the ring. Taking our cue from Figure 3, we hypothesize that the eight-permitted isotopomers can be divided into four groups and assigned to the four observed phenylalanine Raman bands: band 1 corresponds to all ^{12}C aromatic rings; band 2 corresponds to $^{12}C_4{}^{13}C_2$ aromatic rings; band 3 corresponds to $^{12}C_2{}^{13}C_4$ aromatic rings; and band 4 corresponds to all ^{13}C aromatic rings. This hypothesis explains the origin of the four different phenylalanine Raman bands in partially isotopically labeled *E. coli* (Figure 3A).

In order to test this hypothesis, Raman frequencies of the permitted isotopomers of phenylalanine were calculated using a quantum chemical procedure based on density functional theory. The geometric structure of an isolated phenylalanine molecule (Figure S3 of the Supporting Information) was optimized and confirmed as a local minimum on the potential energy surface by diagonalization of the Hessian matrix. The vibrational mode of interest is the Raman-active "ring-breathing" mode (Movie 002 of the Supporting Information). Conformers in which the aromatic ring has rotated about the σ bond that connects it to the remainder of the molecule have, in principle, different Raman frequencies (isotopomers marked "a" and "b" in Figure S4 of the Supporting Information), but the results show that this effect is negligible (± 0.2 cm^{-1}). Figure S4 of the Supporting Information shows Raman frequencies of permitted isotopomers. The ring-breathing mode appears at 1017 cm^{-1} and 980 cm^{-1} for all ^{12}C and all ^{13}C isotopomers, respectively (i.e., with a frequency overestimation of 1.5%, which is within the typical uncertainty for this level of theory and the simplified model of in vivo phenylalanine as an isolated species).[27] The results are clustered in four groups, as isotopic substitution in the C_3 backbone has negligible effect on the Raman frequency of the ring-breathing mode, and this allows unambiguous assignment of the four experimental peaks (Figure 4). This assignment is independent of the precise level of theory: for example, calculations with the Hartree–Fock method, which neglects electron correlation, give identical trends and peak assignments (See Figure S5 of the Supporting Information).

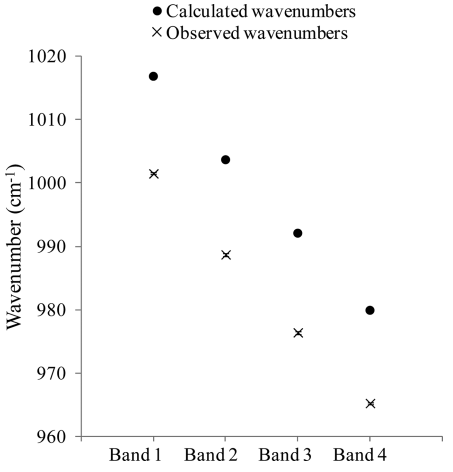

Figure 4. Calculated and observed Raman band positions (wavenumber) of the four phenylalanine Raman bands. Error bars show the standard error of the observed wavenumbers.

dx.doi.org/10.1021/ac302910x | *Anal. Chem.* XXXX, XXX, XXX–XXX

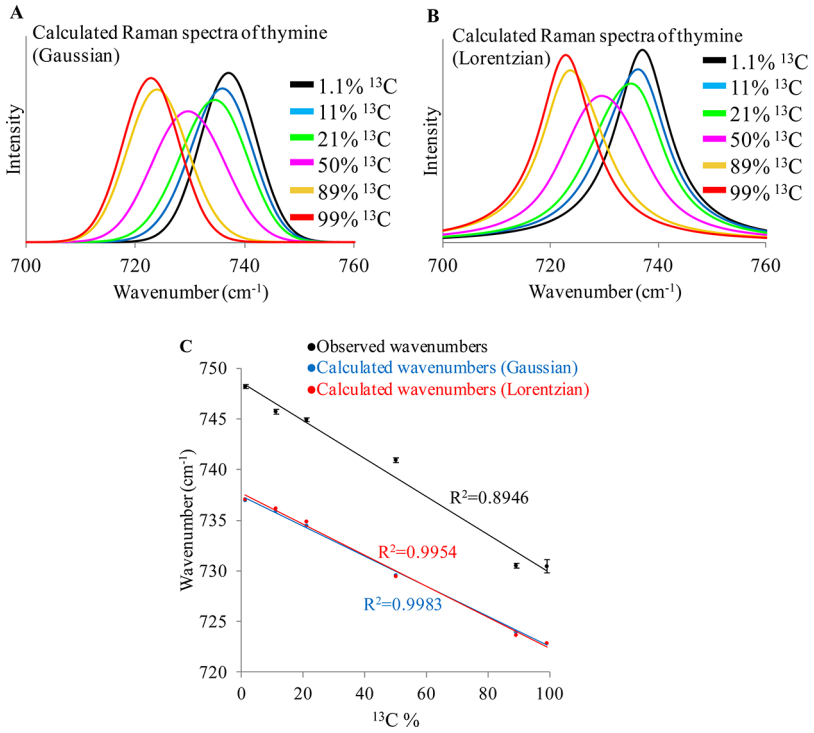

Figure 5. Simulated and observed Raman red shift of the thymine Raman band. (A and B) Simulated thymine Raman spectra using Gaussian and Lorentzian functions show similar gradual red shift with increasing carbon-13 content; (C) a comparison of the Raman red shift was drawn between the simulated and observed spectra with error bars showing the standard error of the observed wavenumbers (Day 5−20).

As described before, red-shift patterns of phenylalanine and thymine are manifestations of their different probability distributions of isotopomers. The aromatic ring in phenylalanine has four permitted isotopomers, giving the probability distribution a four-peak shape. The Raman frequencies of these isotopomers are well-separated; therefore this four-peak probability distribution manifests itself as a four-peak Raman spectrum.

Proposed Mechanism for the Red-Shift Pattern of the Thymine Raman Band. The origin of carbon atoms in the biosynthesis of thymine is more complex than that of phenylalanine. Here, we attempt to demonstrate how increased complexity of the thymine biosynthesis ultimately leads to a red-shift pattern differing from that of phenylalanine. *De novo* synthesis of deoxythymidylate (dTMP) with deoxyuridylate (dUMP) as its immediate precursor will be used as a typical pathway to demonstrate our hypothesis (Figure S2, panel B of the Supporting Information).[26] Oxaloacetate, carbamoyl phosphate, and N^5,N^{10}-methylenetetrahydrofolate provide three, one and one carbon atom(s), respectively. Carbamoyl phosphate is a one-carbon molecule of bicarbonate origin and, therefore, can randomly contribute a ^{12}C or ^{13}C to the thymine biosynthesis. The carbon atom that N^5,N^{10}-methylenetetrahydrofolate contributes could originate from a number of biological molecules; therefore, we consider it to be random. The remaining three carbon atoms come from oxaloacetate, an intermediate in the citric acid cycle. From examination of this cycle, we conclude that oxaloacetate also contains random ratios of ^{13}C and ^{12}C. In the citric acid cycle, the precursors of oxaloacetate are succinate and fumarate. In succinate, neither the two methylene carbon atoms nor the two carboxylic carbon atoms are distinguishable; in fumarate, neither the two alkene carbon atoms nor the two carboxylic carbon atoms are distinguishable. ^{12}C and ^{13}C can randomly enter the cycle in the form of acetyl coenzyme A; they can also randomly leave the cycle in the form of CO_2, owing to the cyclic nature of these reactions and the symmetries of succinate and fumarate. As a result, oxaloacetate can leave the cycle and enter the biosynthesis of thymine with any number of ^{12}C and ^{13}C. Therefore, thymine molecules can carry a random number of ^{12}C and ^{13}C.

A phenylalanine molecule is divided into three modules which can be traced to its origin in glucose, the sole carbon source in growth media (Figure 3B). However, the origin of carbon atoms in thymine is highly diverse and "tracing" them would be difficult, if not impossible. We hypothesize that, owing to the complexity in the origin of carbon atoms, all 32 possible isotopomers of thymine are permitted.

On the basis of this hypothesis, Raman spectra of thymine can be calculated and compared to observation. The structure of the isolated thymine molecule (Figure S6 of the Supporting Information) was optimized using the same method as for phenylalanine. The vibrational mode of interest here is the asymmetric "ring-breathing" vibration (Movie 003 of the Supporting Information). This mode appears at 737 cm^{-1} for the all ^{12}C isotopomer, indicating a discrepancy of 1.3%, which is well within the uncertainties associated with the level of theory and the simplified model of in vivo thymine as an isolated species. The average isotopic shift per ^{13}C substitution at sites a, b, c, d, and e is −4, −1, −3, −6, and −0.1 cm^{-1}, respectively (Figure S6 of the Supporting Information). The Raman band of thymine can be seen as the superposition of the Raman bands of all permitted isotopomers. Each isotopomer has a distinct calculated Raman frequency (Figure S7 of the Supporting Information) and intensity. In order to calculate the intensity profile of the thymine Raman band, a probability for each isotopomer is also needed. The carbon atom provided by

dx.doi.org/10.1021/ac302910x | *Anal. Chem.* XXXX, XXX, XXX−XXX

carbamoyl phosphate can be seen as independent from that provided by N^5,N^{10}-methylenetetrahydrofolate. These two carbon atoms can be also seen as independent from oxaloacetate. The three carbon atoms of oxaloacetate, as described before, can be seen as independent from each other as the result of the citric acid cycle. Therefore, the probability of each isotopomer, as a function of ^{13}C % (see Materials and Methods), can be calculated based on the hypothesis that the isotopic nature of carbon atoms in thymine results from a combination of five independent statistical events. Gaussian and Lorentzian functions were used to calculate Raman bands for the 32 isotopomers with four parameters: observed full width at half-maximum (FWHM), isotopomer probability, calculated Raman frequency, and calculated relative intensity. The final spectra were calculated by adding the 32 Gian or Lorentzian functions together (Figure 5, panels A and B). Peak position (wavenumber) of the calculated thymine Raman spectra were compared with observed values (Figure 5C and Figure S8 of the Supporting Information). Calculated Raman spectra exhibit a linear red shift with increasing ^{13}C content, and no obvious band splitting is seen. This prediction matches the observed red-shift pattern of the thymine band. Gaussian and Lorentzian functions produced virtually identical results.

DISCUSSION

This study describes a novel Raman spectral marker which enables the monitoring of carbon flow from an environmental carbon source, via microorganisms, to single predatory nematodes in a rapid, nondestructive and quantitative manner. This marker is the thymine Raman band, which has a different red-shift pattern from another important Raman spectral marker, the phenylalanine band. A mechanism accounting for this difference is proposed in this study, which is supported by quantum chemical calculation, revealing a dependence of the Raman red shift on biochemistry. This study provides researchers with a new tool for quantifying ^{13}C incorporation at the single-cell level. We have demonstrated that the analysis of the red shifts and changes of the Raman bands can be used to reveal biosynthetic pathways. By revealing this hidden relationship, this study also proves the concept that the SIP-Raman method can be a simple but powerful technique for probing complex biochemical reaction networks.

The slope of the linear regression line for the observed red shift shows that a ±5.3% change in ^{13}C % will shift the thymine band by ±1 cm^{-1} (Figure 5C). Therefore, when the thymine Raman band is used to determine single-cells ^{13}C content, 5.3% can be seen as the resolution of the ^{13}C % measurement with the present Raman equipment used in this study. It could be further improved by using a better spectrometer and finer grating. In comparison with other methods which measure isotopic incorporation, such as mass spectrometry, secondary-ion mass spectrometry, and ultracentrifugation, this resolution is competitive.

It has been shown that the extent of Raman red shift of abundant biological molecules is representative of the extent of ^{13}C-incorporation of the whole cell.[3] Pretreatment of Raman spectra was kept to a minimum to avoid artifacts. Commonly used baseline correction methods should be approached with caution in Raman spectroscopy because the constitution of the "baseline" of a Raman band can be complicated, including fluorescence, neighboring Raman bands, and instrument background. One of the key points is that the Raman shift of the thymine band can be used as a simple indicator of ^{13}C-incorporation in cells without using Raman band intensity or any questionable baseline correction techniques.

On the basis of the collection of single-cell Raman spectra in our laboratory, the thymine Raman band is observed in *C. elegans*, Chinese hamster ovary (CHO) cells, human embryonic stem cells, and some protists, but this band is usually absent in the Raman spectra of bacteria. Interestingly, the thymine band appears in a strain of *Pseudomonas* sp., and this strain is known to have an accumulation of DNA absorbed on its surface.[28] The almost universally observed phenylalanine Raman band will still serve as a quantitative spectral marker for the ^{13}C content at the single-cell level, but when the thymine band is available, it will be more reliable as Raman wavenumbers are more accurate than Raman band intensities. This newly developed method will offer a high-throughput analysis of ^{13}C level in single eukaryotic cells and will help with better understanding of carbon flow and metabolic pathways and permits the analysis of individual levels of the whole foodweb.

ASSOCIATED CONTENT

Supporting Information

Additional information as noted in text. This material is available free of charge via the Internet at http://pubs.acs.org.

AUTHOR INFORMATION

Corresponding Author

*E-mail: w.huang@sheffield.ac.uk. Tel: +44 (0)114 2225796. Fax: +44 (0)114 2225701.

Notes

The authors declare no competing financial interest.

ACKNOWLEDGMENTS

We acknowledge support from the Ministry of Science and Technology of China (MOST 2011IM030100). We thank The University of Sheffield for providing studentships to M.L. and C.M.G., Dr. E. S. Wharfe (University of Sheffield) for the discussion on the prochirality in the citric acid cycle, and Stefan Scheu for financial support and helpful suggestions on the manuscript. We thank Wellsens Biotech Ltd. for technical support, and we also thank Susanne Boening-Klein for her assistance with nematodes.

REFERENCES

(1) Huang, W. E.; Li, M.; Jarvis, R. M.; Goodacre, R.; Banwart, S. A.: Shining Light on the Microbial World: The Application of Raman Microspectroscopy. In *Advances in Applied Microbiology*; Elsevier Academic Press Inc.: San Diego, 2010; Vol. *70*; pp 153−186.

(2) Li, M.; Xu, J.; Romero-Gonzalez, M.; Banwart, S. A.; Huang, W. E. *Curr. Opin. Biotechnol.* **2012**, *23*, 56−63.

(3) Li, M.; Canniffe, D. P.; Jackson, P. J.; Davison, P. A.; FitzGerald, S.; Dickman, M. J.; Burgess, J. G.; Hunter, C. N.; Huang, W. E. *ISME J.* **2012**, *6*, 875−885.

(4) Hall, E. K.; Singer, G. A.; Polzl, M.; Hammerle, I.; Schwarz, C.; Daims, H.; Maixner, F.; Battin, T. J. *ISME J.* **2011**, *5*, 196−208.

(5) Wagner, M. *Annu. Rev. Microbiol.* **2009**, *63*, 411−429.

(6) Haider, S.; Wagner, M.; Schmid, M. C.; Sixt, B. S.; Christian, J. G.; Hacker, G.; Pichler, P.; Mechtler, K.; Muller, A.; Baranyi, C.; Toenshoff, E. R.; Montanaro, J.; Horn, M. *Mol. Microbiol.* **2010**, *77*, 687−700.

(7) Huang, W. E.; Stoecker, K.; Griffiths, R.; Newbold, L.; Daims, H.; Whiteley, A. S.; Wagner, M. *Environ. Microbiol.* **2007**, *9*, 1878−1889.

(8) Huang, W. E.; Ferguson, A.; Singer, A. C.; Lawson, K.; Thompson, I. P.; Kalin, R. M.; Larkin, M. J.; Bailey, M. J.; Whiteley, A. S. *Appl. Environ. Microbiol.* **2009**, *75*, 234−241.

(9) Lugtenberg, B.; Kamilova, F. *Annu. Rev. Microbiol.* **2009**, *63*, 541−556.
(10) Jousset, A. *Environ. Microbiol.* **2012**, *14*, 1830−1843.
(11) Lueders, T.; Wagner, B.; Claus, P.; Friedrich, M. W. *Environ. Microbiol.* **2004**, *6*, 60−72.
(12) Murase, J.; Frenzel, P. *Environ. Microbiol.* **2007**, *9*, 3025−3034.
(13) Kuppardt, S.; Chatzinotas, A.; Kastner, M. *Appl. Environ. Microbiol.* **2010**, *76*, 8222−8230.
(14) Pollierer, M. M.; Langel, R.; Korner, C.; Maraun, M.; Scheu, S. *Ecology Letters* **2007**, *10*, 729−736.
(15) Radajewski, S.; Ineson, P.; Parekh, N. R.; Murrell, J. C. *Nature* **2000**, *403*, 646−649.
(16) Haichar, F. E.; Marol, C.; Berge, O.; Rangel-Castro, J. I.; Prosser, J. I.; Balesdent, J.; Heulin, T.; Achouak, W. *ISME J.* **2008**, *2*, 1221−1230.
(17) Schnider-Keel, U.; Seematter, A.; Maurhofer, M.; Blumer, C.; Duffy, B.; Gigot-Bonnefoy, C.; Reimmann, C.; Notz, R.; Defago, G.; Haas, D.; Keel, C. *J. Bacteriol.* **2000**, *182*, 1215−1225.
(18) Frisch, M. J.; Trucks, G. W.; Schlegel, H. B.; Scuseria, G. E.; Robb, M. A.; Cheeseman, J. R.; Scalmani, G.; Barone, V.; Mennucci, B.; Petersson, G. A.; Nakatsuji, H.; Caricato, M.; Li, X.; Hratchian, H. P.; Izmaylov, A. F.; Bloino, J.; Zheng, G.; Sonnenberg, J. L.; Hada, M.; Ehara, M.; Toyota, K.; Fukuda, R.; Hasegawa, J.; Ishida, M.; Nakajima, T.; Honda, Y.; Kitao, O.; Nakai, H.; Vreven, T.; Montgomery, J. A. Jr.; Peralta, J. E.; Ogliaro, F.; Bearpark, M.; Heyd, J. J.; Brothers, E.; Kudin, K. N.; Staroverov, V. N.; Keith, T.; Kobayashi, R.; Normand, J.; Raghavachari, K.; Rendell, A.; Burant, J. C.; Iyengar, S. S.; Tomasi, J.; Cossi, M.; Rega, N.; Millam, J. M.; Klene, M.; Knox, J. E.; Cross, J. B.; Bakken, V.; Adamo, C.; Jaramillo, J.; Gomperts, R.; Stratmann, R. E.; Yazyev, O.; Austin, A. J.; Cammi, R.; Pomelli, C.; Ochterski, J. W.; Martin, R. L.; Morokuma, K.; Zakrzewski, V. G.; Voth, G. A.; Salvador, P.; Dannenberg, J. J.; Dapprich, S.; Daniels, A. D.; Farkas, O.; Foresman, J. B.; Ortiz, J. V.; Cioslowski, J.; Fox, D. J. *Gaussian 09*, revision C.01; Gaussian, Inc.: Wallingford, CT, 2010.
(19) Duguid, J.; Bloomfield, V. A.; Benevides, J.; Thomas, G. J. *Biophys. J.* **1993**, *65*, 1916−1928.
(20) Duguid, J. G.; Bloomfield, V. A.; Benevides, J. M.; Thomas, G. J. *Biophys. J.* **1995**, *69*, 2623−2641.
(21) Duguid, J. G.; Bloomfield, V. A.; Benevides, J. M.; Thomas, G. J. *Biophys. J.* **1996**, *71*, 3350−3360.
(22) Fodor, S. P. A.; Starr, P. A.; Spiro, T. G. *Biopolymers* **1985**, *24*, 1493−1500.
(23) Deng, H.; Bloomfield, V. A.; Benevides, J. M.; Thomas, G. J. *Biopolymers* **1999**, *50*, 656−666.
(24) Benevides, J. M.; Overman, S. A.; Thomas, G. J. *J. Raman Spectrosc.* **2005**, *36*, 279−299.
(25) Mathlouthi, M.; Seuvre, A. M.; Koenig, J. L. *Carbohydr. Res.* **1984**, *134*, 23−38.
(26) Stryer, L. *Biochemistry*, 4th ed.; W.H. Freeman: New York, 1995.
(27) Irikura, K. K.; Johnson, R. D.; Kacker, R. N. *J. Phys. Chem. A* **2005**, *109*, 8430−8437.
(28) Andrews, J. S.; Rolfe, S. A.; Huang, W. E.; Scholes, J. D.; Banwart, S. A. *Environ. Microbiol.* **2010**, *12*, 2496−2507.